

This is a repository copy of *Remarkable Levels of ^{15}N Polarization Delivered through SABRE Into Unlabeled Pyridine, Pyrazine or Metronidazole Enable Single Scan NMR Quantification at the mM Level.*

White Rose Research Online URL for this paper:

<https://eprints.whiterose.ac.uk/160690/>

Version: Accepted Version

Article:

Fekete, Marianna orcid.org/0000-0003-4869-0912, Ahwal, Fadi and Duckett, Simon B. orcid.org/0000-0002-9788-6615 (2020) Remarkable Levels of ^{15}N Polarization Delivered through SABRE Into Unlabeled Pyridine, Pyrazine or Metronidazole Enable Single Scan NMR Quantification at the mM Level. *Journal of Physical Chemistry B*. jp-2020-02583e. ISSN 1520-5207

<https://doi.org/10.1021/acs.jpcb.0c02583>

Reuse

Items deposited in White Rose Research Online are protected by copyright, with all rights reserved unless indicated otherwise. They may be downloaded and/or printed for private study, or other acts as permitted by national copyright laws. The publisher or other rights holders may allow further reproduction and re-use of the full text version. This is indicated by the licence information on the White Rose Research Online record for the item.

Takedown

If you consider content in White Rose Research Online to be in breach of UK law, please notify us by emailing eprints@whiterose.ac.uk including the URL of the record and the reason for the withdrawal request.

Remarkable Levels of N Polarization Delivered through SABRE Into Unlabeled Pyridine, Pyrazine or Metronidazole Enable Single Scan NMR Quantification at the mM Level

Marianna Fekete, Fadi Ahwal, and Simon B Duckett

J. Phys. Chem. B, **Just Accepted Manuscript** • DOI: 10.1021/acs.jpcc.0c02583 • Publication Date (Web): 08 May 2020

Downloaded from pubs.acs.org on May 12, 2020

Just Accepted

“Just Accepted” manuscripts have been peer-reviewed and accepted for publication. They are posted online prior to technical editing, formatting for publication and author proofing. The American Chemical Society provides “Just Accepted” as a service to the research community to expedite the dissemination of scientific material as soon as possible after acceptance. “Just Accepted” manuscripts appear in full in PDF format accompanied by an HTML abstract. “Just Accepted” manuscripts have been fully peer reviewed, but should not be considered the official version of record. They are citable by the Digital Object Identifier (DOI®). “Just Accepted” is an optional service offered to authors. Therefore, the “Just Accepted” Web site may not include all articles that will be published in the journal. After a manuscript is technically edited and formatted, it will be removed from the “Just Accepted” Web site and published as an ASAP article. Note that technical editing may introduce minor changes to the manuscript text and/or graphics which could affect content, and all legal disclaimers and ethical guidelines that apply to the journal pertain. ACS cannot be held responsible for errors or consequences arising from the use of information contained in these “Just Accepted” manuscripts.

1
2
3
4
5
6
7 Remarkable levels of ^{15}N polarization delivered
8
9
10
11 through SABRE into unlabeled pyridine, pyrazine or
12
13
14
15 metronidazole enable single scan NMR
16
17
18
19 quantification at the mM level.
20
21
22
23

24 *Marianna Fekete, Fadi Ahwal and Simon B. Duckett**

25
26
27
28 *University of York, Department of Chemistry, Heslington, York, YO10 5DD (UK)*
29
30

31 KEYWORDS. ^{15}N polarization, SABRE, *parahydrogen*
32
33
34
35
36
37

38 ABSTRACT. While many drugs and metabolites contain nitrogen, harnessing their diagnostic ^{15}N -
39
40 NMR signature for their characterization is underutilized due to inherent detection difficulties.
41
42 Here we demonstrate how precise ultra-low field SABRE (± 0.2 mG) in conjunction *para*-hydrogen
43
44 and an iridium precatalyst of the form $\text{IrCl}(\text{COD})(\text{NHC})$ with the co-ligand *d*₉-benzylamine allows
45
46 the natural abundance ^{15}N NMR signatures of pyridine, pyrazine, metronidazole and acetonitrile
47
48 to be readily detected at 9.4 T in single NMR observations through $>50\%$ ^{15}N polarization levels.
49
50 These signals allow rapid and precise reagent quantification via a response that varies linearly over
51
52 the 2 mM to 70 mM concentration range.
53
54
55
56
57
58
59
60

Introduction

Hyperpolarization methods have been shown to dramatically improve the sensitivity of Nuclear Magnetic Resonance (NMR) and Magnetic Resonance Imaging (MRI)¹⁻² in a process that involves increasing the purity of the magnetic states they detect. Signal amplification by reversible exchange (SABRE) reflects one such method. It harnesses the nuclear spin order of *para*-hydrogen (*p*-H₂)^{3,4,5} and is a consequence of the pioneering work of Weitekamp⁶ and Eisenberg.⁷ For SABRE to operate, the symmetry of *p*-H₂ is first broken by temporarily placing it into a metal complex so that the new hydride ligands which result couple distinctly to NMR active spins within the ligand sphere of the product. A process of reversible binding then allows a suitable substrate to become hyperpolarized through what is a catalytic process that transfers nuclear spin order within the complex rather than achieving a change in chemical identity.^{3,5} Typically this process takes place in a specified magnetic field that is often called the polarization transfer field (PTF) and can be selected to optimize efficiency.⁸⁻⁹ The selection of this field is made according to the chemical shift difference that exists between the interacting nuclear spins and their spin-spin couplings^{10,11} in a process that has been accurately modelled.¹² As the active SABRE catalyst may break the symmetry of the two protons that were initially located in *p*-H₂ through chemical or magnetic inequivalence effects the process of catalysis can be complex.^{5, 13} This is because for spin order transfer from the *p*-H₂ derived hydride ligands to take place, the receiving ligand nuclei must exhibit different spin-spin couplings to these two protons.

Knowledge of this behavior has influenced SABRE catalyst design¹⁴ and the resulting sensitization process has enabled the easy NMR detection of low-abundance inorganic species.¹³ Other studies have used deuterated co-ligands to improve the spin-order yields in SABRE by

1
2
3 reducing waste through the focusing of polarization transfer into fewer receptor sites.¹⁵ When this
4
5 is achieved in conjunction with ²H labelling, the associated extension of nuclear spin-order lifetime
6
7 has proven to be particularly beneficial as de-coherence within the SABRE catalyst reflects one
8
9 route to reduce the overall processes efficiency.¹⁶ These two effects combine to extend the duration
10
11 over which signals remain visible to NMR. as in classical terms one T_1 period is associated with a
12
13 63% destruction of the hard-won polarization level. Not surprisingly, the extended lifetimes
14
15 associated with molecular singlet states¹⁷⁻²¹ and their derivatives, feature extensively in
16
17 hyperpolarization research as one goal is often to study *in vivo* reactivity.²² In further
18
19 developments, Tessari *et al.* have shown how ¹H-SABRE can achieve precise analyte
20
21 quantification at low substrate loadings by the involvement of a slow exchanging co-ligand.²³⁻²⁴
22
23 Furthermore, Iali *et al* extended SABRE to the hyperpolarization of primary amines through
24
25 catalysts of the form $[\text{Ir}(\text{H})_2(\text{IMes})(\text{amine})_3]\text{Cl}$,²⁵ and it was noted that sterically hindered amines
26
27 which failed to bind efficiently benefited by the addition of smaller NCMe which enables the
28
29 formation of $[\text{Ir}(\text{H})_2(\text{IMes})(\text{aniline})_2(\text{NCMe})]\text{Cl}$.²⁶ The successful use of amines reflects an
30
31 important boost to SABRE because the hyperpolarized NH response can be used to sensitize other
32
33 molecules through proton exchange.²⁵ More recently developments of this ligand design route have
34
35 enabled the hyperpolarization of pyruvate and acetate.²⁷⁻²⁸
36
37
38
39
40
41

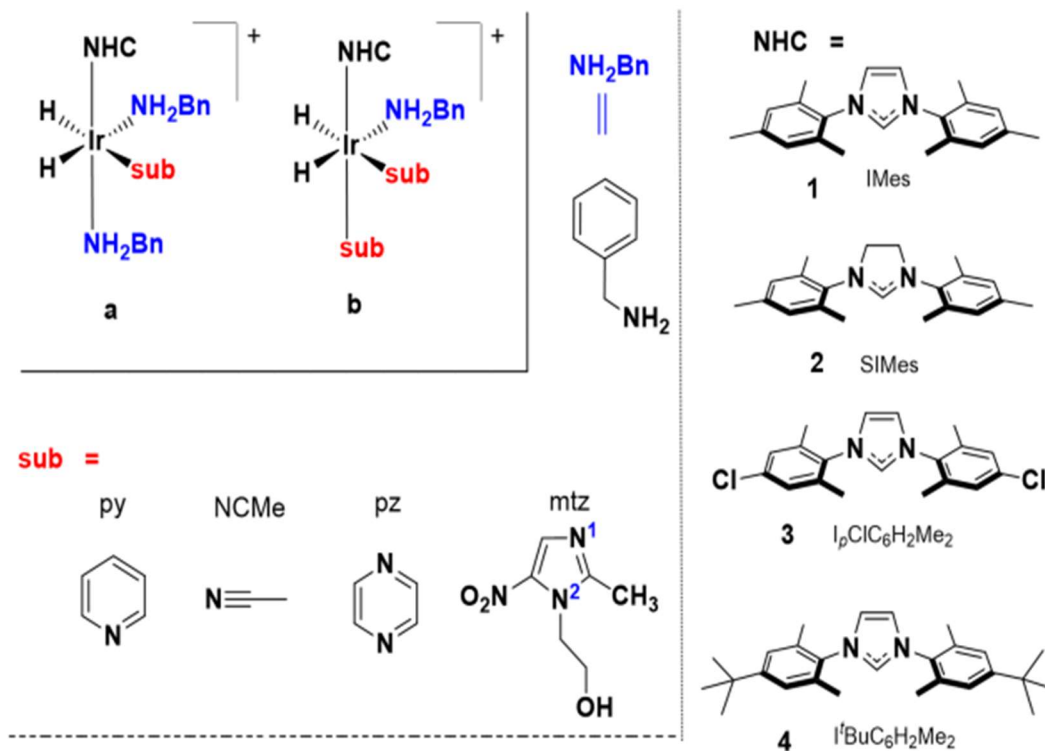
42 Normally, though the detection of ¹⁵N by NMR is even more challenging than that of ¹H because
43
44 of its 0.36% natural abundance and low magnetogyric ratio. ¹⁵N detection is, however, needed for
45
46 the characterization of important nucleobases, nucleosides, nucleotides, peptides, proteins and
47
48 transition metal complexes. In addition, as the T_1 of ¹⁵N can exceed many minutes, magnetic state
49
50 lifetimes can approach those of positron emission tomography.²⁹⁻³³ It is not therefore surprising
51
52 that ¹⁵N hyperpolarization reflected an early target of both spontaneous³ and radio frequency
53
54
55
56
57
58
59
60

1
2
3 driven SABRE.³⁴ Warren *et al.* refined these methods through SABRE SHEATH³⁵⁻³⁶ to deliver
4 20% ¹⁵N polarization in metronidazole.³⁷ Several alternative radio frequency strategies have also
5
6 been exemplified³⁸⁻⁴⁰ and given the goal of *in vivo* SABRE, water soluble SABRE catalysts have
7
8 also been described⁴¹⁻⁴² with the MRI detection of a ¹⁵N response illustrated.⁴² Here though we
9
10 seek to demonstrate how amines as co-ligands can enable the highly efficient ¹⁵N polarization of
11
12 a range of target substrates (sub) via SABRE catalysis through [Ir(H)₂(**1**)(sub)₂(BnNH₂)]Cl (**a**) or
13
14 [Ir(H)₂(**1**)(sub)(BnNH₂)₂]Cl (**b**) of Scheme 1 in order to improve on the potential of SABRE
15
16 approach to achieve *in vivo* MRI detection.
17
18
19
20
21
22
23

24 Results

25 Hyperpolarization of the ¹⁵N NMR signal of pyridine.

26
27 We start by considering non-labelled pyridine at a 35 mM concentration because of its wide use
28
29 in early SABRE research^{3,4, 13} in conjunction with the precatalyst [IrCl(COD)(*h*₂₂-**1**)]⁴³ (5 mM) of
30
31 Scheme 1. Our experimental measurements involved examining an NMR tube containing
32
33 methanol-*d*₄ solutions of these reagents under 3 bar (absolute) pressure of *p*-H₂ at 99% purity. The
34
35 *p*-H₂ gas is first dissolved by shaking the NMR tube whilst it is located in a pre-set magnetic field
36
37 that lies between ±1 mG to ±140 G for ~10 seconds (relative to the main NMR magnets field
38
39 orientation). Subsequently, the sample is placed in a 9.4 T magnet where the final NMR signal
40
41 detection step occurs.
42
43
44
45
46
47
48
49
50
51
52
53
54
55
56
57
58
59
60



Scheme 1. Chemical structures of complexes, substrates and ligands.

Under these conditions, the SABRE catalyst $[\text{Ir}(\text{H})_2(h_{22-1})(\text{py})_3]\text{Cl}$ forms and a ^1H NMR signal gain of 1452-fold can be seen for the *ortho*-proton resonance of free pyridine that is present in solution after transfer from a 60 G field. This polarization transfer step takes 10 seconds to complete and the resulting polarization level (P_{H}) is 4.65% (P_x reflects the percentage polarization associated with nuclei x). In this case, the catalyst breaks the symmetry of the two *p*-H₂ derived protons through magnetic inequivalence effects and hence spin order transfer flows optimally within the equatorial plane that contains the hydride ligands into bound pyridine.⁴⁴ For ^{15}N , however, the large *trans* two bond ^1H - ^{15}N coupling of ~ 19 Hz^{45,9,35, 46} that connects these hydride ligands to nitrogen in $[\text{Ir}(\text{H})_2(h_{22-1})(\text{py})_3]\text{Cl}$ enables the efficient transfer of polarization at an approximate -1 mG field that is of the same sense to the main 9.4 T observation field. The

1
2
3 consequence of this process is a 39200 fold ($\pm 2\%$) ^{15}N -NMR signal gain which means the
4
5 corresponding $P_{^{15}\text{N}}$ value is 12.9% ($\pm 2\%$). Hence this unlabeled 35 mM sample of pyridine can be
6
7 detected by ^{15}N NMR spectroscopy in a single scan NMR measurement at a magnetic field of 9.4
8
9 T with a signal to noise ratio 11 using a routine inverse detection probe.

11
12
13 **Establishing that the co-ligand benzylamine is beneficial to the hyperpolarization of the ^{15}N**
14
15 **NMR signal of pyridine.**

16
17
18 When the co-ligand d_7 -benzylamine ($d_7\text{-BnNH}_2$) was added to such a sample, at an initial
19
20 concentration of 17.5 mM, it proved to rapidly convert into its d_9 -benzylamine isotopologue.
21
22 Consequently, we refer to $d_9\text{-BnND}_2$ throughout this manuscript even though $d_7\text{-BnNH}_2$ is actually
23
24 added to the samples. The resulting ^1H NMR spectra reveal that in addition to this labelling change,
25
26 two new inorganic species are formed which yield pairs of hydride ligand signals at δ -22.14 and
27
28 -22.58, and δ -23.34 and -23.73 respectively. These hydride ligand signals arise from $[\text{Ir}(\text{H})_2(h_{22}\text{-}$
29
30 **1)($d_9\text{-BnND}_2$)(py) $_2$ Cl** and $[\text{Ir}(\text{H})_2(h_{22}\text{-1})(d_9\text{-BnND}_2)_2(\text{py})]\text{Cl}$ respectively that are present in
31
32 solution in the ratio 2.6 : 1. The two complexes contain inequivalent hydride ligands that differ
33
34 from one another according to the identity of the axial ligands in the complex as detailed in Scheme
35
36 1 and the SI. Furthermore, as their proportions match the value seen when a similar sample is
37
38 created by the initial addition of benzylamine and H_2 to $[\text{IrCl}(\text{COD})(h_{22}\text{-1})]$, but before pyridine
39
40 addition takes place, it can be concluded that these two complexes are in equilibrium. Hence the
41
42 separation of their roles in the underlying SABRE process is impractical, but we note it would be
43
44 expected that both will contribute to this process. In addition, it is important to recognize that both
45
46 of these complexes contain chemically and magnetically distinct hydride ligands. The result of this
47
48 change is that spin-order transfer can now proceed into ligands that lie *trans* and *cis* to hydride,
49
50 which means that spin dilution, associated with polarization of the axial ligands, is expected and
51
52
53
54
55
56
57
58
59
60

1
2
3 this will reduce the SABRE signal gains that are seen for the free substrate.⁴⁴ Hence, the
4 involvement of polarization transfer protecting d_9 -BnND₂ which limits spin-order wastage should
5 be of significant benefit to the SABRE outcome.
6
7
8
9

10
11 When the resulting d_9 -BnND₂ solutions were examined for SABRE, the ¹H NMR response
12 resulting from this mixture of catalysts proved to contain a free pyridine *ortho* proton resonance
13 that was 880-fold (± 50) larger than expected after transfer from a 60 G field. As this gain is smaller
14 than the value achieved by [Ir(H)₂(*h*₂₂-1)(py)₃]Cl we can conclude that under these conditions the
15 [Ir(H)₂(*h*₂₂-1)(d_9 -BnND₂)(py)₂]Cl/[Ir(H)₂(*h*₂₂-1)(d_9 -BnND₂)₂(py)]Cl mixture is actually less
16 efficient at hyperpolarizing the ¹H NMR signals of pyridine than [Ir(H)₂(*h*₂₂-1)(py)₃]Cl. More
17 notable though is the fact that the corresponding ¹⁵N NMR spectrum contains a signal that is
18 indicative of a P_{15N} value of 18% (53300 ± 6000 fold) in conjunction with a PTF of approximately
19 -1 mG (Figure 1a). This reflects a 27% improvement in SABRE efficiency when compared to that
20 achieved by [Ir(H)₂(*h*₂₂-1)(py)₃]Cl and confirms that there is a benefit to using the co-ligand d_9 -
21 benzylamine when seeking ¹⁵N polarization.
22
23
24
25
26
27
28
29
30
31
32
33
34
35
36

37 Upon changing to [IrCl(*d*₂₂-1)(COD)], and completing a similar series of d_9 -BnND₂ promoted
38 measurements, the levels of signal gain seen in the pyridine *ortho* proton ¹H NMR signal rises to
39 1324-fold, although the ¹⁵N polarization level proved to be unaffected. Hence, while catalyst
40 deuteration is not successful at improving SABRE ¹⁵N activity, it is able to improve the level of
41 ¹H signal gain because of reduced spin order wastage and improved ¹H relaxation.¹⁶ This suggests
42 that low-field ¹⁵N-relaxation within the catalyst is not improved.
43
44
45
46
47
48
49
50
51

52 While it is well known that the optimum SABRE catalyst changes with the identity of the
53 substrate, it has been clearly demonstrated here that there is also a further dependence on the
54
55
56
57
58
59
60

1
2
3 efficiency of SABRE transfer within a given substrate according to whether ^1H or ^{15}N is the target.
4
5 The optimum rate of ligand exchange for ^1H transfer has been proposed by Barskiy to be 4.5 s^{-1} in
6
7 complexes of the type $[\text{Ir}(\text{H})_2(h_{22}\text{-1})(\text{py})_3]\text{Cl}$. Consequently, the rate of pyridine substrate
8
9 dissociation in $[\text{Ir}(\text{H})_2(h_{22}\text{-1})(\text{py})_2(d_9\text{-BnND}_2)]\text{Cl}$ in methanol- d_4 solution was determined using
10
11 the EXSY method and found to be 0.06 s^{-1} at 268 K. This value increases to 1.04 s^{-1} upon warming
12
13 to at 298 K, and 2.1 s^{-1} at 308 K. Our associated SABRE measurements reveal that the
14
15 corresponding ^1H NMR signal gains change from 600-fold, through 4530-fold to 3550-fold at the
16
17 308 K setting. Hence it appears that a rate closer to 1.04 s^{-1} is optimal for ^1H transfer into pyridine
18
19 using this catalyst. Our experiments also reveal that there is a 30% growth in efficiency of ^{15}N
20
21 polarization for pyridine on moving from 268 K to 298 K, and a further 22% improvement on
22
23 moving to 308 K from 298 K. Consequently, we can confirm that the two different nuclei are best
24
25 served with different rates of ligand exchange.
26
27
28
29
30
31
32
33
34
35
36
37
38
39
40
41
42
43
44
45
46
47
48
49
50
51
52
53
54
55
56
57
58
59
60

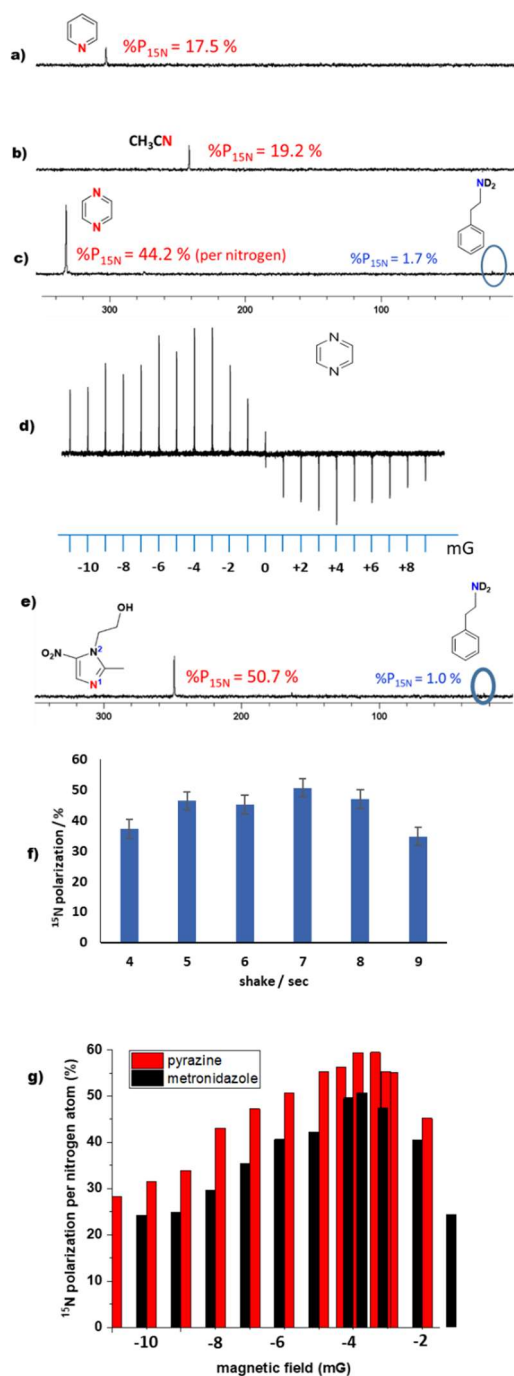


Figure 1. Polarized ^{15}N NMR signals of a) pyridine, b) acetonitrile, c) and d) pyrazine and e) metronidazole. Levels indicated in figure alongside agent. In d), the series of ^{15}N NMR signals for pyrazine vary in intensity according to the magnitude of the polarization transfer field. f) Shake time dependence of $P_{15\text{N}}$ level in metronidazole with $[\text{IrCl}(d_{34}\text{-4})(\text{COD})]$. g) $P_{15\text{N}}$ level for metronidazole (black) and pyrazine (red) in a 10 mm sample tube as a function of PTF magnitude.

Hyperpolarization of the ^{15}N NMR signal of acetonitrile.

In order to develop this method further, acetonitrile was tested at a similar 35 mM concentration in conjunction with the SABRE catalyst $[\text{Ir}(\text{H})_2(h_{22}\text{-}\mathbf{1})(\text{NCMe})_3]\text{Cl}$. This catalyst also relies on magnetic inequivalence to break the symmetry of the hydride ligands and it yields a ^1H NMR signal gain of just 83-fold per methyl proton in the unbound acetonitrile present in solution after transfer at 298 K from a 70 G field. The SABRE derived ^{15}N NMR signal gain for CH_3CN was found to be far more substantial, at 41800 ± 6000 fold (14% polarization) after transfer from an approximate -1 mG field.

Acetonitrile hyperpolarization was then studied in conjunction with 3.6 equivalents of the co-ligand d_9 -benzylamine relative to a 5.2 mM iridium concentration. Both $[\text{Ir}(\text{H})_2(d_9\text{-BnND}_2)_2(\text{NCMe})(h_{22}\text{-}\mathbf{1})]\text{Cl}$ and $[\text{Ir}(\text{H})_2(d_9\text{-BnND}_2)_3(h_{22}\text{-}\mathbf{1})]\text{Cl}$ form in these experiments, in a 2:1 ratio. They both possess chemically distinct hydride ligands. The resulting ^1H NMR response after SABRE showed an improved ^1H NMR signal gain of 160-fold per proton for CH_3CN while its ^{15}N polarization level rose to 19% (Figure 1b).

For the corresponding ^2H labeled precatalyst $[\text{IrCl}(d_{22}\text{-}\mathbf{1})(\text{COD})]$, the ^1H NMR signal again improves further to 367-fold per proton in accordance with reduced spin dilution that arises as a consequence of hydride ligand chemical inequivalence in $[\text{Ir}(\text{H})_2(d_9\text{-BnND}_2)_2(\text{NCMe})(h_{22}\text{-}\mathbf{1})]\text{Cl}$ and $[\text{Ir}(\text{H})_2(d_9\text{-BnND}_2)_3(h_{22}\text{-}\mathbf{1})]\text{Cl}$, but now the achieved $P_{15\text{N}}$ level fell to 10%. Hence ^2H -catalyst labelling of the NHC ligand is now detrimental to the ^{15}N polarization level. In this case, the appreciable concentration of $[\text{Ir}(\text{H})_2(d_9\text{-BnNH}_2)_2(\text{NCMe})(d_{22}\text{-}\mathbf{1})]\text{Cl}$, where there will be coupling between the ^2H labels of the NHC and the ^{15}N of NCMe, could result in the reduction in ^{15}N -SABRE efficiency. Barskiy's observations that in micro-Tesla transfer fields scalar relaxation of

1
2
3 the second kind⁴⁷ associated with the quadrupolar ^{14}N - ^{13}C interaction limits the level of ^{13}C
4 polarization under SABRE support this view.⁴⁸ The gain in ^1H signal intensity relative to the
5 situation with h_{22} -**1** is, however, consistent with a reduction in polarization transfer into this ligand
6 through deuteration and an extension of the hydride ligands relaxation times.¹⁴
7
8
9
10
11
12
13

14 **Hyperpolarization of the ^{15}N NMR signal of pyrazine.**

15
16
17 We next consider pyrazine (pz). This substrate was tested by taking 5.2 mM methanol- d_4
18 solutions of $[\text{IrCl}(\text{COD})(h_{22}\text{-1})]$ that contained a 7-fold excess of pz under 3 bar of $p\text{-H}_2$. The
19 resulting ^1H NMR signal gain for pz was now 900 fold per proton (2.9 % polarization) and a $P_{15\text{N}}$
20 value of 16% (± 2 , per nitrogen used throughout) was observed after transfer from -3mG.
21
22
23
24
25

26 Studies with added $h_7\text{-BnND}_2$ resulted in a ^1H NMR signal gain of 566 fold (0.8%) and a ^{15}N
27 signal gain of 12% due to the associated spin dilution effects. However, when $d_9\text{-BnND}_2$ and $h_{22}\text{-}$
28 **1** were used with a PTF of 60 G, radiation damping resulted with ^1H signal detection. In order to
29 aid the analysis, this artifact could be suppressed if a less efficient PTF of 120 G was used. Analysis
30 under these conditions was used to deduce that the corresponding P_{H} level is 13.5% (± 0.6) per
31 proton for a 60 G measurement while for ^{15}N it was 38% (per nitrogen). The ^1H NMR signal gain
32 grew further to 30.9% (± 0.7) when $[\text{IrCl}(d_{22}\text{-1})(\text{COD})]$ was used but the corresponding ^{15}N signal
33 response fell in intensity meaning that scalar relaxation of the second kind is again important We
34 also tested the related SIMes containing precatalyst $[\text{IrCl}(\text{COD})(\mathbf{2})]$ ⁴⁹ with pyrazine and discovered
35 that a $P_{15\text{N}}$ value of 15.8% could be achieved without a co-ligand. Samples containing both $d_7\text{-}$
36 benzylamine and pyrazine yield $[\text{Ir}(\text{H})_2(\text{pz})_2(d_9\text{-BnND}_2)(h_{22}\text{-2})]\text{Cl}$ and $[\text{Ir}(\text{H})_2(d_9\text{-}$
37 $\text{BnND}_2)_2(\text{pz})(h_{22}\text{-2})]\text{Cl}$ in the ratio 2:1 and a $P_{15\text{N}}$ value of 44.2% via PTF from an approximate -
38 1.9 mG field (Figure 1c). This falls to 31.8% with d_{22} -SIMes in agreement with a role for ^2H -drive
39
40
41
42
43
44
45
46
47
48
49
50
51
52
53
54
55
56
57
58
59
60

1
2
3 relation in the SABRE catalyst at low field. Figure 1d shows that the sign of the polarization
4 transfer field, relative to that of the main observation field affects the measured ^{15}N pz signal gains.
5
6 This is because upon moving the sample slowly between the points of polarization transfer and
7
8 measurement if it experiences a zero-field point there is a loss in spin order due to relaxation at
9
10 this point.
11
12
13

14
15 The rate of pyrazine dissociation from $[\text{Ir}(\text{H})_2(\text{pz})_2(d_9\text{-BnND}_2)(h_{22}\text{-2})]\text{Cl}$ was determined using
16
17 the EXSY method to be 0.33 s^{-1} at 268 K when the ^1H NMR signal gain is 660 fold. This rate
18
19 increases to 1.8 s^{-1} at 298 K where the ^1H signal gain is 2200 fold. Our experiments reveal a 20%
20
21 growth in efficiency of ^{15}N polarization on moving from 268 K to 298 K for pyrazine as a
22
23 consequence of this rate increase which is faster than that of pyridine loss in the related complex
24
25 $[\text{Ir}(\text{H})_2(h_{22}\text{-1})(\text{py})_2(d_9\text{-BnND}_2)]\text{Cl}$. This kinetic difference is consistent with the relative ^{15}N
26
27 polarization efficiencies of 44.2% and 18% respectively.
28
29
30
31
32

33 **Hyperpolarization of the ^{15}N NMR signal of metronidazole.**

34
35 Biologically significant metronidazole^{50, 51} has been well-studied by Chekmenev *et al.*^{52, 53, 54, 55}
36
37 We conducted control measurements for 5.2 mM methanol- d_4 solutions of $[\text{IrCl}(\text{COD})(h_{22}\text{-1})]$ and
38
39 $[\text{IrCl}(\text{COD})(h_{22}\text{-2})]$ with a 7-fold excess of metronidazole relative to iridium and a 3 bar pressure
40
41 of $p\text{-H}_2$ but failed to see significant polarization in either sample. However, once a 3.6-fold excess
42
43 of d_7 -benzylamine was added, polarization transfer to proton and ^{15}N was readily seen with both
44
45 precursors. For $[\text{IrCl}(\text{COD})(h_{22}\text{-1})]$ the $P_{^{15}\text{N}}$ value was 22% whilst for $[\text{IrCl}(\text{COD})(h_{22}\text{-2})]$ it was
46
47 24% (transfer at -2 mG and 2% $P_{^{15}\text{N}}$ seen for d_7 -benzylamine itself). When the ^2H labeled versions
48
49 of these catalysts, $[\text{IrCl}(\text{COD})(d_{22}\text{-1})]$ or $[\text{IrCl}(\text{COD})(d_{22}\text{-2})]$, were used, these $P_{^{15}\text{N}}$ values rose to
50
51
52
53
54
55
56
57
58
59
60

27%. In all cases the reaction with d_9 -benzylamine and metronidazole formed $[\text{Ir}(\text{H})_2(\text{mtz})_2(d_9\text{-BnND}_2)(\text{NHC})]\text{Cl}$ and $[\text{Ir}(\text{H})_2(d_9\text{-BnND}_2)_2(\text{mtz})(\text{NHC})]\text{Cl}$ with the ratio being 1.4:1 for $d_{22}\text{-2}$.

Data was now collected on the $d_{22}\text{-2}$ system to demonstrate that the PTF value can be used to control which of the two substrates present in solution receives polarization. This effect serves to illustrate how selectivity can be introduced into the analysis of mixtures if peak overlap is an issue (see SI). Furthermore, a catalyst change to $[\text{IrCl}(\text{COD})(d_{34}\text{-4})]$ increased the N_1 value to 51% for metronidazole with 4% polarization being achieved on N_2 and 1% on d_9 -benzylamine.

The rates of metronidazole dissociation from the resulting complex $[\text{Ir}(\text{H})_2(\text{mtz})_2(d_9\text{-BnND}_2)(d_{34}\text{-4})]\text{Cl}$ were determined in methanol- d_4 solution at 268, 298 and 308 K by the EXSY method as being 0.80 s^{-1} , 2.37 s^{-1} and 5.5 s^{-1} respectively. For the ^1H signal gain, 298 K proved to be best, yielding an enhancement of 856-fold. We now see an 80% growth in efficiency of ^{15}N polarization on moving from 268 K to 298 K, but the $P_{15\text{N}}$ values falls to just 18% at 308 K. Hence increasing the ligand exchange rate beyond 2.4 s^{-1} seems detrimental.

	Nucleus (PTF)	1	$d_{22}\text{-1}$	2	$d_{22}\text{-2}$	3	$d_{16}\text{-3}$	4	$d_{34}\text{-4}$	Error, %, \pm
	Signal Gain (P)									
Pyrazine	^1H (120 G) / fold	137 2	3151	2220	6028	2533	558	556	673	4
	^{15}N (% , as indicated PTF mG)	38 (-3)	35 (-3)	44 (-1.9)	37 (-5)	26 (-2)	31 (-4)	32 (-5)	28 (-3)	2
Metronidazole- N_1	^1H (60 G) / fold	326	474	560	446	814	1038	676	856	5
	^{15}N (%, at PTF of -2 mG)	22	27	24	27	23	23	32	51	3

Table 1. Absolute value of ^1H (total proton) and ^{15}N NMR (per site) signal enhancement levels for pyrazine and metronidazole at the specified PTF for samples with d_9 -benzylamine as a co-ligand.

Using higher proportions of *p*-H₂ to improve the NMR signal gain.

A series of measurements were then completed on metronidazole using a 10 mm NMR tube to deploy a larger excess of *p*-H₂ in conjunction with [IrCl(COD)(*d*₃₄-4)] and *d*₉-benzylamine. A slight increase in ¹⁵N polarization level to 54% results alongside a reduction in response variability to 2%. Consequently, as shown in Figure 1g, a -3.6 mG PTF can be deduced as being optimal. Similar 10 mm measurements were then made for pyridine with [IrCl(COD)(*h*₂₂-1), acetonitrile with [IrCl(COD)(*h*₂₂-1) and pyrazine with [IrCl(COD)(*h*₂₂-2) in the presence of *d*₉-benzylamine. These studies saw the *P*_{15N} level for pyridine increase to 48% at 4 bar *p*-H₂ pressure. When acetonitrile was examined a 30.7% *P*_{15N} level was reached, but for pyrazine it became 59.4% per nitrogen. Further increases in the pyrazine % *P*_{15N} level can be achieved through reagent dilution such that when an initial 5 mM solution of [IrCl(COD)(*h*₂₂-2)] with a 3.6-fold excess of *d*₉-benzylamine and 7-fold excess of pyrazine based on iridium is diluted 10 fold, the *P*_{15N} value increases to 79%; the S/N ratio in this case is 11.3. In this case the effect is directly analogous to increasing the volume of *p*-H₂ available.

Quantification of reagent concentrations at the mM level through a SABRE enhanced ¹⁵N signal

Once we had ascertained how to achieve these polarization levels, we tested how the magnitude of the pyridine, pyrazine and metronidazole response varied as a function of substrate concentrations between 2.2 and 70 mM. These solutions were made up by simply diluting a stock solution with an initial catalyst, *d*₇-benzylamine and substrate concentration of 10 mM, 36 mM and 70 mM respectively. We discovered that there was a linear variation in signal response in each case as detailed in Figure 2.

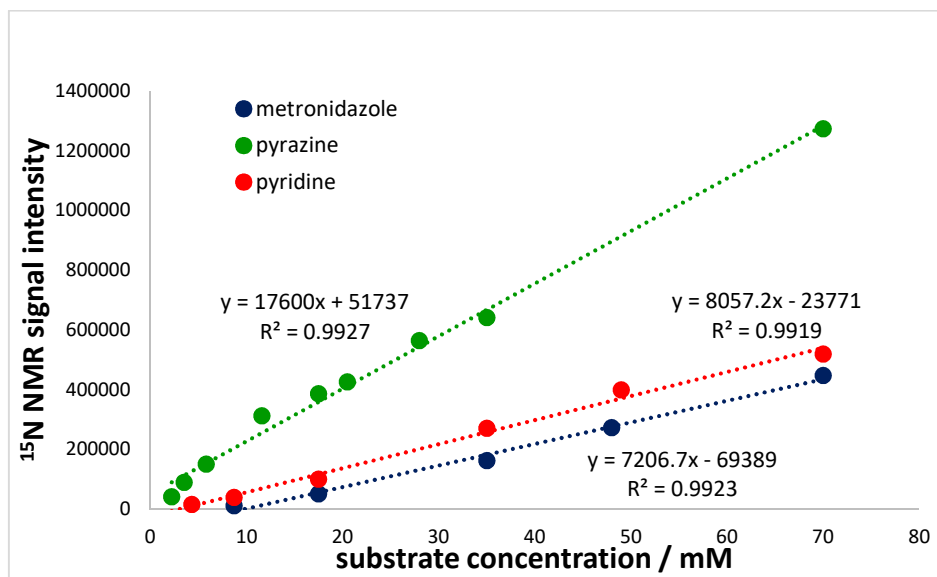


Figure 2. Raw signal intensity resulting from a series of hyperpolarized ^{15}N NMR spectra of pyridine, metronidazole and pyrazine as a function of their concentration. The polarization transfer field was optimized for each substrate. The stock solution of the sample ($[\text{Ir}] = 6.5\text{mM}$, substrate = 70mM , and $22.7\text{mM } d_9\text{-BnND}_2$) was diluted during these measurements, from 70mM substrate to 2.2mM substrate concentration. The straight lines result from linear regression analysis and the square of the sample correlation coefficient $-R^2$ -confirms linear behavior.

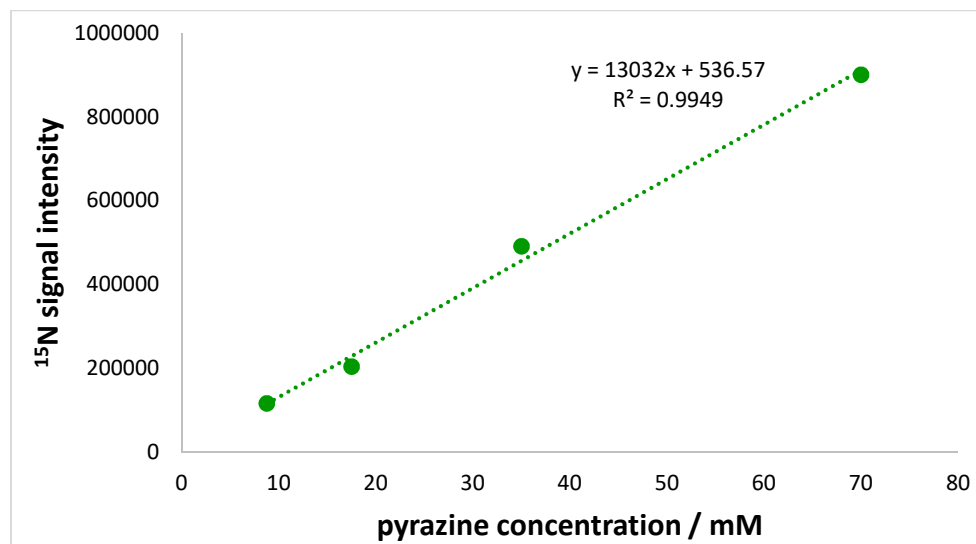
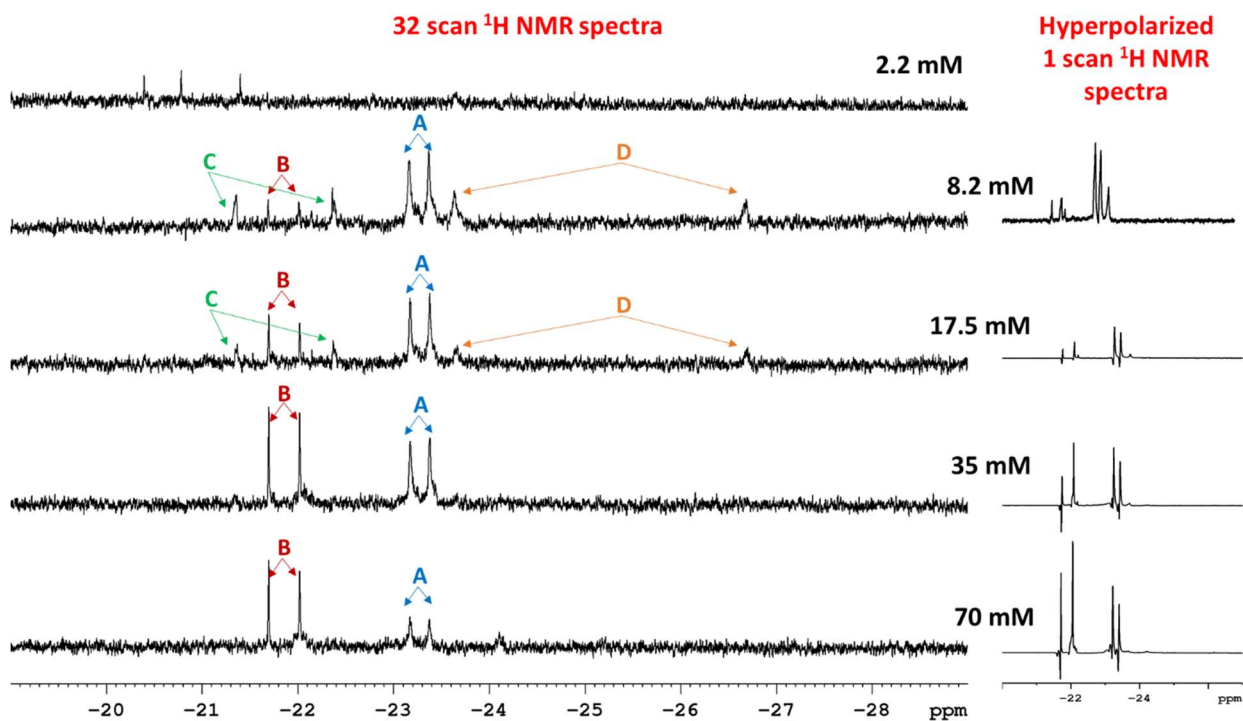


Figure 3. Raw signal intensity resulting from a series of hyperpolarized ^{15}N NMR spectra of pyrazine as a function of its concentration. The polarization transfer field used was -1.9mG . The concentration of the $[\text{Ir}]$ -precatalyst ($[\text{IrCl}(\text{COD})(h_{22}\text{-2})]$) was kept constant at 6.5mM . 3.6 equivalents of $d_9\text{-BnND}_2$ were added relative to metal. Subsequently, the concentration of added

pyrazine was varied from 8.2 mM to 70 mM. Straight line behavior results thereby confirming that the absolute concentration of pyrazine can be estimated from such data.

In second series of studies we maintained a constant iridium and co-ligand concentration whilst changing the pyrazine concentration. A linear change in ^{15}N signal intensity was again observed (Figure 3) despite in this case observing some changes in catalyst form. The hydride region of the polarized NMR spectra confirm that both $[\text{Ir}(\text{H})_2(\text{pz})(d_9\text{-BnND}_2)_2(h_{22}\text{-2})]\text{Cl}$ (**A**) and $[\text{Ir}(\text{H})_2(\text{pz})_2(d_9\text{-BnND}_2)(h_{22}\text{-2})]\text{Cl}$ (**B**) of Figure 4 form with the former being favored at low pyrazine loadings. As the concentration of pyrazine decrease, the amount of the formed complex **B** decreases and as a result of it the ^{15}N polarization of pyrazine linearly decrease as well. This suggest that the main SABRE – ^{15}N catalyst is the type **B** complex. We are currently exploring this behavior in more detail. These data therefore confirm that substrate detection and quantification is feasible via a ^{15}N SABRE signal (see SI).



1
2
3 Figure 4: Effect of pyrazine loading on catalyst speciation when methanol- d_4 solutions of
4 $[\text{IrCl}(\text{COD})(h_{22}\text{-2})]$ are examined with d_9 -BnND₂ and pyrazine in the presence of p -H₂ seen through
5 the hydride region of the corresponding ¹H NMR spectra. Left, thermally equilibrated NMR
6 spectra, right initial SABRE enhanced NMR spectra. Species **A** and **B** are defined in the text whilst
7
8
9
10
11
12
13 **C** is $\text{Ir}(\text{H})_2(\text{Cl})(d_9\text{-BnND}_2)(\text{pz})(h_{22}\text{-2})$ and **D** $[\text{Ir}(\text{H})_2(d_9\text{-BnND}_2)(\text{methanol-}d_4)(h_{22}\text{-2})]\text{Cl}$.

14 15 16 17 **Conclusions**

18
19 We have described here how the addition of the co-ligand d_9 -benzylamine to a precatalyst based
20 on $[\text{IrCl}(\text{NHC})(\text{COD})]$ under p -H₂ results in very high levels of ¹⁵N polarization in a range of
21 substrates. The high field measurements were made in conjunction with the simple shake and drop
22 approach, and it takes approximately 17 seconds to complete a measurement. In the case of the
23 substrates pyridine and acetonitrile, $[\text{IrCl}(h_{22}\text{-1})(\text{COD})]$ led to $P_{15\text{N}}$ values of 48% and 30.9%
24 respectively after transfer from an appropriate mG field. In contrast, a 59.4 $P_{15\text{N}}$ value for pyrazine
25 was achieved using the precatalyst $[\text{IrCl}(h_{22}\text{-2})(\text{COD})]$. These reactions involve the formation of a
26 range of SABRE catalysts of the form $[\text{Ir}(\text{H})_2(\text{sub})_2(d_9\text{-BnND}_2)(\text{NHC})]\text{Cl}$ and $[\text{Ir}(\text{H})_2(\text{sub})(d_9\text{-}$
27 $\text{BnND}_2)_2(\text{NHC})]\text{Cl}$ which are in equilibrium.

28
29
30
31
32
33
34
35
36
37
38
39
40
41
42
43
44
45
46
47
48
49
50
51
52
53
54
55
56
57
58
59
60
Previous studies have established that using deuterated NHC ligands ($d_{22}\text{-1}$ and $d_{22}\text{-2}$) improve
SABRE hyperpolarization transfer efficiency into methyl nicotinate. This improvement is based on
an extension of the hydride ligands relaxation times.¹⁴ Studies here confirm that higher $P_{1\text{H}}$ values
result in all cases in support of this benefit. However, deuteration is not beneficial for ¹⁵N transfer
in pyridine, pyrazine and acetonitrile. Barskiy's observations that in micro-Tesla transfer fields
scaler relaxation of the second kind⁴⁷ associated with the quadrupolar ¹⁴N-¹³C interaction limits
the level of ¹³C polarization under SABRE offer a route to explain this view.⁴⁸ For metronidazole,

1
2
3 however, an improved value of 54% on N₁ results with *d*₉-benzylamine and [IrCl(COD)(*d*₃₄-4)]
4 which when compared to that seen with precatalyst [IrCl(COD)(*h*₃₄-4)]. Hence, ²H labelling of the
5 catalyst can also be of significant benefit to *P*_{15N}.
6
7

8
9
10 The rates of ligand exchange were also assessed alongside the collection of variable temperature
11 SABRE data. It was found that the rate of optimum ligand exchange was slower than that found
12 for ¹H transfer despite the larger ¹H-¹⁵N transfer coupling. We are currently exploring this behavior
13 in more detail.
14
15

16
17
18 Data was also presented that was collected from larger 10 mm NMR tubes using a 4 bar pressure
19 of *p*-H₂. This acted to increase the relative excess of the hyperpolarization fuel *p*-H₂ relative to the
20 substrate and proved to result in greatly improved response reproducibility. Consequently, results
21 demonstrated that a polarization transfer field precision of ±0.2 mG is needed for optimal ¹⁵N
22 transfer. In addition, ~50% ¹⁵N polarization levels could now be achieved in pyrazine, pyridine or
23 metronidazole, which makes them all highly detectable even at low concentration.
24
25

26
27
28 In order to demonstrate an analytical use for these ¹⁵N signals, results were presented to
29 demonstrate that the magnitude of the resulting NMR response scales linearly with concentration
30 over the range 2.2 to 70 mM. This means that such SABRE-derived data can be used to quantify
31 their amount in solution when set against a suitable reference trace. Tessari have completed a
32 growing range of studies which demonstrate ¹H detection levels can be linked to both speciation
33 and quantity²³⁻²⁴, while we have described how ¹³C signals in glucose can be linked to amount.⁵⁶
34
35 These studies employed a methylated triazol co-ligand to simplify the exchange kinetics in order
36 to produce the necessary linear response. We were unable to benchmark our data with that of the
37 triazol co-ligand as it is not commercially available. We did, however, test *d*₆-dmsO which is
38
39
40
41
42
43
44
45
46
47
48
49
50
51
52
53
54
55
56
57
58
59
60

1
2
3 finding widespread use as a co-ligand for the sensitization of weakly binding substrates as an
4
5 alternative. As detailed in the SI the corresponding SABRE performance was degraded.
6

7
8 It is therefore clear that SABRE offers a simple and yet efficient route to analyte quantification
9
10 by ^{15}N NMR spectroscopy. Not surprisingly, we predict these results will therefore be of benefit
11
12 if you wish to use ^{15}N NMR as a characterization tool, or simply to quantify precise, and yet low,
13
14 levels of nitrogen containing drugs that are present in solution or to collect ^{15}N -MRI data.
15
16
17
18
19

20 ASSOCIATED CONTENT

21
22
23 **Supporting Information.** Experimental details, NMR data and hyperpolarization details
24
25

26 AUTHOR INFORMATION

27 28 29 **Corresponding Author**

30
31
32 *Email for S. B. D.: simon.duckett@york.ac.uk
33
34

35 **Author Contributions**

36
37
38 The manuscript was written through contributions of all authors. All authors have given approval
39
40 to the final version of the manuscript. ‡
41
42

43 **Funding Sources**

44
45
46 Financial support from the Wellcome Trust (Grants 092506 and 098335), the MRC
47
48 (MR/M008991/1) and the University of York is gratefully acknowledged. **Notes**
49
50

51 Any additional relevant notes should be placed here.
52
53

54 **ACKNOWLEDGMENT**

We thank Peter Rayner for providing some of the complexes used in this work.

REFERENCES

1. Dumez, J. N., Perspectives on hyperpolarised solution-state magnetic resonance in chemistry. *Magn. Reson. Chem.* **2017**, *55* (1), 38-46.
2. Kovtunov, K. V.; Pokochueva, E. V.; Salnikov, O. G.; Cousin, S. F.; Kurzbach, D.; Vuichoud, B.; Jannin, S.; Chekmenev, E. Y.; Goodson, B. M.; Barskiy, D. A.; Koptug, I. V., Hyperpolarized NMR Spectroscopy: d-DNP, PHIP, and SABRE Techniques. *Chem.-Asian J.* **2018**, *13* (15), 1857-1871.
3. Adams, R. W.; Aguilar, J. A.; Atkinson, K. D.; Cowley, M. J.; Elliott, P. I. P.; Duckett, S. B.; Green, G. G. R.; Khazal, I. G.; López-Serrano, J.; Williamson, D. C., Reversible Interactions with para-Hydrogen Enhance NMR Sensitivity by Polarization Transfer. *Science* **2009**, *323* (5922), 1708-1711.
4. Atkinson, K. D.; Cowley, M. J.; Elliott, P. I. P.; Duckett, S. B.; Green, G. G. R.; López-Serrano, J.; Whitwood, A. C., Spontaneous Transfer of Parahydrogen Derived Spin Order to Pyridine at Low Magnetic Field. *J. Am. Chem. Soc.* **2009**, *131* (37), 13362-13368.
5. Adams, R. W.; Duckett, S. B.; Green, R. A.; Williamson, D. C.; Green, G. G. R., A theoretical basis for spontaneous polarization transfer in non-hydrogenative parahydrogen-induced polarization. *Journal of Chemical Physics* **2009**, *131* (19), 194505.
6. Bowers, C. R.; Weitekamp, D. P., Transformation of symmetrization order to nuclear-spin magnetization by chemical-reaction and nuclear-magnetic-resonance. *Phys. Rev. Lett.* **1986**, *57* (21), 2645-2648.
7. Eisenberg, R., Parahydrogen-induced polarization - a new spin on reactions with H₂. *Accounts Chem. Res.* **1991**, *24* (4), 110-116.
8. Dücker, E. B.; Kuhn, L. T.; Münnemann, K.; Griesinger, C., Similarity of SABRE field dependence in chemically different substrates. *J. Magn. Reson.* **2012**, *214*, 159-165.
9. Cowley, M. J.; Adams, R. W.; Atkinson, K. D.; Cockett, M. C. R.; Duckett, S. B.; Green, G. G. R.; Lohman, J. A. B.; Kerssebaum, R.; Kilgour, D.; Mewis, R. E., Iridium N-Heterocyclic Carbene Complexes as Efficient Catalysts for Magnetization Transfer from para-Hydrogen. *J. Am. Chem. Soc.* **2011**, *133* (16), 6134-6137.
10. Green, R. A.; Adams, R. W.; Duckett, S. B.; Mewis, R. E.; Williamson, D. C.; Green, G. G. R., The theory and practice of hyperpolarization in magnetic resonance using parahydrogen. *Progress in Nuclear Magnetic Resonance Spectroscopy* **2012**, *67*, 1-48.
11. Korchak, S. E.; Ivanov, K. L.; Yurkovskaya, A. V.; Vieth, H. M., Para-hydrogen induced polarization in multi-spin systems studied at variable magnetic field. *Phys. Chem. Chem. Phys.* **2009**, *11* (47), 11146-11156.
12. Barskiy, D. A.; Knecht, S.; Yurkovskaya, A. V.; Ivanov, K. L., SABRE: Chemical kinetics and spin dynamics of the formation of hyperpolarization. *Progress in Nuclear Magnetic Resonance Spectroscopy* **2019**, *114-115*, 33-70.

13. Fekete, M.; Bayfield, O.; Duckett, S. B.; Hart, S.; Mewis, R. E.; Pridmore, N.; Rayner, P. J.; Whitwood, A., Iridium(III) Hydrido N-Heterocyclic Carbene–Phosphine Complexes as Catalysts in Magnetization Transfer Reactions. *Inorg. Chem.* **2013**, *52* (23), 13453-13461.
14. Rayner, P. J.; Norcott, P.; Appleby, K. M.; Iali, W.; John, R. O.; Hart, S. J.; Whitwood, A. C.; Duckett, S. B., Fine-tuning the efficiency of para-hydrogen-induced hyperpolarization by rational N-heterocyclic carbene design. *Nature Communications* **2018**, *9* (1), 4251.
15. Fekete, M.; Rayner, P. J.; Green, G. G. R.; Duckett, S. B., Harnessing polarisation transfer to indazole and imidazole through signal amplification by reversible exchange to improve their NMR detectability. *Magn. Reson. Chem.* **2017**, *55* (10), 944-957.
16. Rayner, P. J.; Burns, M. J.; Oлару, A. M.; Norcott, P.; Fekete, M.; Green, G. G. R.; Highton, L. A. R.; Mewis, R. E.; Duckett, S. B., Delivering strong H-1 nuclear hyperpolarization levels and long magnetic lifetimes through signal amplification by reversible exchange. *Proc. Natl. Acad. Sci. U. S. A.* **2017**, *114* (16), E3188-E3194.
17. Roy, S. S.; Norcott, P.; Rayner, P. J.; Green, G. G. R.; Duckett, S. B., A Hyperpolarizable H-1 Magnetic Resonance Probe for Signal Detection 15 Minutes after Spin Polarization Storage. *Angew. Chem.-Int. Edit.* **2016**, *55* (50), 15642-15645.
18. Roy, S. S.; Norcott, P.; Rayner, P. J.; Green, G. G. R.; Duckett, S. B., A Simple Route to Strong Carbon-13 NMR Signals Detectable for Several Minutes. *Chem.-Eur. J.* **2017**, *23* (44), 10496-10500.
19. Theis, T.; Ortiz, G. X.; Logan, A. W. J.; Claytor, K. E.; Feng, Y.; Huhn, W. P.; Blum, V.; Malcolmson, S. J.; Chekmenev, E. Y.; Wang, Q.; Warren, W. S., Direct and cost-efficient hyperpolarization of long-lived nuclear spin states on universal N-15(2)-diazirine molecular tags. *Sci. Adv.* **2016**, *2* (3), 7.
20. Stevanato, G.; Hill-Cousins, J. T.; Hakansson, P.; Roy, S. S.; Brown, L. J.; Brown, R. C. D.; Pileio, G.; Levitt, M. H., A Nuclear Singlet Lifetime of More than One Hour in Room-Temperature Solution. *Angew. Chem.-Int. Edit.* **2015**, *54* (12), 3740-3743.
21. Dumez, J. N., Perspective on long-lived nuclear spin states. *Molecular Physics*, 11.
22. Levitt, M. H., Long live the singlet state! *J. Magn. Reson.* **2019**, *306*, 69-74.
23. Sellies, L.; Reile, I.; Aspers, R.; Feiters, M. C.; Rutjes, F.; Tessari, M., Parahydrogen induced hyperpolarization provides a tool for NMR metabolomics at nanomolar concentrations. *Chem. Commun.* **2019**, *55* (50), 7235-7238.
24. Eshuis, N.; Hermkens, N.; van Weerdenburg, B. J. A.; Feiters, M. C.; Rutjes, F.; Wijmenga, S. S.; Tessari, M., Toward Nanomolar Detection by NMR Through SABRE Hyperpolarization. *J. Am. Chem. Soc.* **2014**, *136* (7), 2695-2698.
25. Iali, W.; Rayner, P. J.; Duckett, S. B., Using para-hydrogen to hyperpolarize amines, amides, carboxylic acids, alcohols, phosphates, and carbonates. *Science Advance* **2018**, *4* (1).
26. Iali, W.; Rayner, P. J.; Alshehri, A.; Holmes, A. J.; Ruddlesden, A. J.; Duckett, S. B., Direct and indirect hyperpolarisation of amines using parahydrogen. *Chem. Sci.* **2018**, *9* (15), 3677-3684.
27. Gemeinhardt, M. E.; Limbach, M. N.; Gebhardt, T. R.; Eriksson, C. W.; Eriksson, S. L.; Lindale, J. R.; Goodson, E. A.; Warren, W. S.; Chekmenev, E. Y.; Goodson, B. M., "Direct" (13) C Hyperpolarization of (13) C-Acetate by MicroTesla NMR Signal Amplification by Reversible Exchange (SABRE). *Angew Chem Int Ed Engl* **2020**, *59* (1), 418-423.

- 1
2
3 28. Iali, W.; Roy, S. S.; Tickner, B.; Ahwal, F.; Kennerley, A. J.; Duckett, S. B.,
4 Hyperpolarising Pyruvate through Signal Amplification by Reversible Exchange (SABRE).
5 *Angew. Chem.-Int. Edit.* **2019**, *58* (30), 10271-10275.
- 6 29. Durst, M.; Chiavazza, E.; Haase, A.; Aime, S.; Schwaiger, M.; Schulte, R. F., alpha-
7 Trideuteromethyl ¹⁵N glutamine: A Long-Lived Hyperpolarized Perfusion Marker. *Magn.*
8 *Reson. Med.* **2016**, *76* (6), 1900-1904.
- 9 30. Cudalbu, C.; Comment, A.; Kurdzesau, F.; van Heeswijk, R. B.; Uffmann, K.; Jannin, S.;
10 Denisov, V.; Kirik, D.; Gruetter, R., Feasibility of in vivo N-15 MRS detection of hyperpolarized
11 N-15 labeled choline in rats. *Phys. Chem. Chem. Phys.* **2010**, *12* (22), 5818-5823.
- 12 31. Gabellieri, C.; Reynolds, S.; Lavie, A.; Payne, G. S.; Leach, M. O.; Eykyn, T. R.,
13 Therapeutic target metabolism observed using hyperpolarized ¹⁵N choline. *J Am Chem Soc*
14 **2008**, *130* (14), 4598-9.
- 15 32. Jagtap, A. P.; Kaltschnee, L.; Glogglar, S., Hyperpolarization of N-15-pyridinium and N-
16 15-aniline derivatives by using parahydrogen: new opportunities to store nuclear spin
17 polarization in aqueous media. *Chem. Sci.* **2019**, *10* (37), 8577-8582.
- 18 33. Harris, T.; Gamliel, A.; Uppala, S.; Nardi-Schreiber, A.; Sosna, J.; Gomori, J. M.; Katz-
19 Brull, R., Long-lived N-15 Hyperpolarization and Rapid Relaxation as a Potential Basis for
20 Repeated First Pass Perfusion Imaging - Marked Effects of Deuteration and Temperature.
21 *Chemphyschem* **2018**, *19* (17), 2148-2152.
- 22 34. Atkinson, K. D.; Cowley, M. J.; Duckett, S. B.; Elliott, P. I. P.; Green, G. G. R.; Lopez-
23 Serrano, J.; Khazal, I. G.; Whitwood, A. C., Para-Hydrogen Induced Polarization without
24 Incorporation of Para-Hydrogen into the Analyte. *Inorg. Chem.* **2009**, *48* (2), 663-670.
- 25 35. Theis, T.; Truong, M. L.; Coffey, A. M.; Shchepin, R. V.; Waddell, K. W.; Shi, F.;
26 Goodson, B. M.; Warren, W. S.; Chekmenev, E. Y., Microtesla SABRE Enables 10% Nitrogen-
27 15 Nuclear Spin Polarization. *J. Am. Chem. Soc.* **2015**, *137* (4), 1404-1407.
- 28 36. Truong, M. L.; Theis, T.; Coffey, A. M.; Shchepin, R. V.; Waddell, K. W.; Shi, F.;
29 Goodson, B. M.; Warren, W. S.; Chekmenev, E. Y., N-15 Hyperpolarization by Reversible
30 Exchange Using SABRE-SHEATH. *J. Phys. Chem. C* **2015**, *119* (16), 8786-8797.
- 31 37. Colell, J. F. P.; Logan, A. W. J.; Zhou, Z.; Shchepin, R. V.; Barskiy, D. A.; Ortiz, G. X.;
32 Wang, Q.; Malcolmson, S. J.; Chekmenev, E. Y.; Warren, W. S.; Theis, T., Generalizing,
33 Extending, and Maximizing Nitrogen-15 Hyperpolarization Induced by Parahydrogen in
34 Reversible Exchange. *The Journal of Physical Chemistry C* **2017**, *121* (12), 6626-6634.
- 35 38. Theis, T.; Truong, M.; Coffey, A. M.; Chekmenev, E. Y.; Warren, W. S., LIGHT-
36 SABRE enables efficient in-magnet catalytic hyperpolarization. *J. Magn. Reson.* **2014**, *248*, 23-
37 26.
- 38 39. Svyatova, A.; Skovpin, I. V.; Chukanov, N. V.; Kovtunov, K. V.; Chekmenev, E. Y.;
39 Pravdivtsev, A. N.; Hovener, J. B.; Koptuyug, I. V., N-15 MRI of SLIC-SABRE Hyperpolarized
40 N-15-Labelled Pyridine and Nicotinamide. *Chem.-Eur. J.* **2019**, *25* (36), 8465-8470.
- 41 40. Pravdivtsev, A. N.; Yurkovskaya, A. V.; Zimmermann, H.; Vieth, H. M.; Ivanov, K. L.,
42 Enhancing NMR of insensitive nuclei by transfer of SABRE spin hyperpolarization. *Chemical*
43 *Physics Letters* **2016**, *661*, 77-82.
- 44 41. Kidd, B. E.; Gesiorski, J. L.; Gemeinhardt, M. E.; Shchepin, R. V.; Kovtunov, K. V.;
45 Koptuyug, I. V.; Chekmenev, E. Y.; Goodson, B. M., Facile Removal of Homogeneous SABRE
46 Catalysts for Purifying Hyperpolarized Metronidazole, a Potential Hypoxia Sensor. *The Journal*
47 *of Physical Chemistry C* **2018**, *122* (29), 16848-16852.
- 48
49
50
51
52
53
54
55
56
57
58
59
60

- 1
2
3 42. Skovpin, I. V.; Svyatova, A.; Chukanov, N.; Chekmenev, E. Y.; Kovtunov, K. V.;
4 Koptuyug, I. V., N-15 Hyperpolarization of Dalfampridine at Natural Abundance for Magnetic
5 Resonance Imaging. *Chem.-Eur. J.* **2019**, *25* (55), 12694-12697.
- 6 43. Torres, O.; Martín, M.; Sola, E., Labile N-Heterocyclic Carbene Complexes of Iridium.
7 *Organometallics* **2009**, *28* (3), 863-870.
- 8 44. Fekete, M.; Bayfield, O.; Duckett, S. B.; Hart, S.; Mewis, R. E.; Pridmore, N.; Rayner, P.
9 J.; Whitwood, A., Iridium(III) Hydrido N-Heterocyclic Carbene-Phosphine Complexes as
10 Catalysts in Magnetization Transfer Reactions. *Inorganic Chemistry* **2013**, *52* (23), 13453-
11 13461.
- 12 45. Mewis, R. E.; Atkinson, K. D.; Cowley, M. J.; Duckett, S. B.; Green, G. G. R.; Green, R.
13 A.; Highton, L. A. R.; Kilgour, D.; Lloyd, L. S.; Lohman, J. A. B.; Williamson, D. C., Probing
14 signal amplification by reversible exchange using an NMR flow system. **2014**, *52* (7), 358-369.
- 15 46. Jiang, W.; Lumata, L.; Chen, W.; Zhang, S.; Kovacs, Z.; Sherry, A. D.; Khemtong, C.,
16 Hyperpolarized ¹⁵N-pyridine Derivatives as pH-Sensitive MRI Agents. *Scientific Reports* **2015**,
17 *5*, 9104.
- 18 47. Pyper, N. C., Theory of scalar relaxation of the second kind. II. *Molecular Physics* **1971**,
19 *21* (6), 961-976.
- 20 48. Barskiy, D. A.; Shchepin, R. V.; Tanner, C. P. N.; Colell, J. F. P.; Goodson, B. M.; Theis,
21 T.; Warren, W. S.; Chekmenev, E. Y., The Absence of Quadrupolar Nuclei Facilitates Efficient
22 ¹³C Hyperpolarization via Reversible Exchange with Parahydrogen. *ChemPhysChem* **2017**, *18*
23 (12), 1493-1498.
- 24 49. Kelly Iii, R. A.; Clavier, H.; Giudice, S.; Scott, N. M.; Stevens, E. D.; Bordner, J.;
25 Samardjiev, I.; Hoff, C. D.; Cavallo, L.; Nolan, S. P., Determination of N-Heterocyclic Carbene
26 (NHC) Steric and Electronic Parameters using the [(NHC)Ir(CO)₂Cl] System. *Organometallics*
27 **2008**, *27* (2), 202-210.
- 28 50. Kizaka-Kondoh, S.; Konse-Nagasawa, H., Significance of nitroimidazole compounds and
29 hypoxia-inducible factor-1 for imaging tumor hypoxia. *Cancer Science* **2009**, *100* (8), 1366-
30 1373.
- 31 51. Procissi, D.; Claus, F.; Burgman, P.; Kozirowski, J.; Chapman, J. D.; Thakur, S. B.;
32 Matei, C.; Ling, C. C.; Koutcher, J. A., In vivo ¹⁹F Magnetic Resonance Spectroscopy and
33 Chemical Shift Imaging of Tri-Fluoro-Nitroimidazole as a Potential Hypoxia Reporter in Solid
34 Tumors. *Clinical Cancer Research* **2007**, *13* (12), 3738-3747.
- 35 52. Barskiy, D. A.; Shchepin, R. V.; Coffey, A. M.; Theis, T.; Warren, W. S.; Goodson, B.
36 M.; Chekmenev, E. Y., Over 20% ¹⁵N Hyperpolarization in Under One Minute for
37 Metronidazole, an Antibiotic and Hypoxia Probe. *J. Am. Chem. Soc.* **2016**, *138* (26), 8080-8083.
- 38 53. Shchepin, R. V.; Jaigirdar, L.; Theis, T.; Warren, W. S.; Goodson, B. M.; Chekmenev, E.
39 Y., Spin Relays Enable Efficient Long-Range Heteronuclear Signal Amplification by Reversible
40 Exchange. *J. Phys. Chem. C* **2017**, *121* (51), 28425-28434.
- 41 54. Shchepin, R. V.; Jaigirdar, L.; Chekmenev, E. Y., Spin-Lattice Relaxation of
42 Hyperpolarized Metronidazole in Signal Amplification by Reversible Exchange in Micro-Tesla
43 Fields. *J. Phys. Chem. C* **2018**, *122* (9), 4984-4996.
- 44 55. Kidd, B. E.; Gesiorski, J. L.; Gemeinhardt, M. E.; Shchepin, R. V.; Kovtunov, K. V.;
45 Koptuyug, I. V.; Chekmenev, E. Y.; Goodson, B. M., Facile Removal of Homogeneous SABRE
46 Catalysts for Purifying Hyperpolarized Metronidazole, a Potential Hypoxia Sensor. *J. Phys.*
47 *Chem C* **2018**, *122* (29), 16848-16852.
- 48
49
50
51
52
53
54
55
56
57
58
59
60

1
2
3 56. Richardson, P. M.; Iali, W.; Roy, S. S.; Rayner, P. J.; Halse, M. E.; Duckett, S. B., Rapid
4 C-13 NMR hyperpolarization delivered from para-hydrogen enables the low concentration
5 detection and quantification of sugars. *Chem. Sci.* **2019**, *10* (45), 10607-10619.
6
7
8
9
10
11
12
13
14
15
16
17
18
19
20
21
22
23
24
25
26
27
28
29
30
31
32
33
34
35
36
37
38
39
40
41
42
43
44
45
46
47
48
49
50
51
52
53
54
55
56
57
58
59
60